



Kinetic Modeling of Low Temperature Epitaxy Growth of SiGe Using Disilane and Digermane

M. Kolahdouz,^{a,z} A. Salemi, M. Moeen, M. Östling,^{*} and H. H. Radamson

School of Information and Communication Technology, KTH (Royal Institute of Technology), Kista 16640, Sweden

Low temperature epitaxy (LTE) in Chemical Vapor Deposition (CVD) refers to 350–650°C interval. This temperature range is critical for this process since the thermal and lattice mismatch (or strain relaxation) issues diminish in advanced BiCMOS processing. The modeling of the epitaxy process is a vital task to increase the understanding the growth process and to design any desired device structure. In this study, an empirical model for Si₂H₆/Ge₂H₆-based LTE of SiGe is developed and compared with experimental work. The model can predict the number of free sites on Si surface, growth rate of Si and SiGe, and the Ge content at low temperatures. A good agreement between the model and the experimental data is obtained.

© 2012 The Electrochemical Society. [DOI: 10.1149/2.jes113689] All rights reserved.

Manuscript submitted December 28, 2011; revised manuscript received January 30, 2012. Published February 16, 2012.

SiGe epitaxy growth has always been an important step in device processing in both micro-^{1–3} and opto-electronics⁴ due to the strain engineering and bandgap narrowing in SiGe/Si heterojunctions. Recently, new application of SiGe/Si heterostructures for infra-red detectors^{5,6} and thermoelectrical devices^{7,8} converts them to an attractive system for many industrial applications. For these applications, low temperature epitaxy (LTE) in CVD (350–650°C) has attracted attention because of the fact that the vulnerable parts of CMOS and BiCMOS structures are preserved at this thermal budget. This eases the prioritizing of different steps in the processing flow. Achieving a very high quality epitaxial SiGe is crucial for these applications.

Plenty of experimental results have been presented on the issues regarding integration of LTE SiGe layers for different applications;^{9–12} meanwhile, remarkably fewer reports are available about the modeling of the epitaxy process.^{13–15} Another important point is that at low temperatures (below 600°C), the traditional precursors e.g. silane (SiH₄) and dichlorosilane (SiH₂Cl₂) are not applicable. This is because of higher activation energy required for breaking Si–H (or Si–Cl) bonds in traditional sources, e.g. SiH₄ and SiH₂Cl₂, compared to Si–Si in disilane (Si₂H₆) and trisilane (Si₃H₈). Nowadays, higher order hydrides gas sources are mainly used for epitaxy growth at temperature range below 550°C. A similar argument may apply here for germane (GeH₄) and digermane (Ge₂H₆) as germanium gas sources. In this case, high quality SiGe layers can be grown at low temperatures, however, the price issue may come forward for the epitaxy process.

In this study, an empirical model for LTE of SiGe in a reduced pressure chemical vapor deposition (RPCVD) using disilane (Si₂H₆) and digermane (Ge₂H₆) is established. The model can predict the number of free sites on Si surface, growth rate of Si and SiGe, and the Ge content at low temperature. The model demonstrates a decent correspondence with the experimental data.

Experimental

The epitaxial layers were grown on blanket Si(100) substrates in an ASM Epsilon 2000 RPCVD reactor at temperature range between 400 to 600°C. Disilane (Si₂H₆) and 10% digermane (Ge₂H₆) in H₂ were used as Si and Ge sources, respectively.

Different partial pressures of Si₂H₆ (P_{Si₂H₆}) and Ge₂H₆ (P_{Ge₂H₆}) were chosen to verify the validity of the model. The hydrogen partial pressure has been considered as an important point for the thermodynamics and gas kinetics in the reactor. This parameter has been altered to achieve different partial pressures of the precursors.

The Ge content and the layer thickness of deposited SiGe layers were measured directly by high resolution X-ray diffraction

(HRXRD). These data were obtained from simulation of the rocking curves by using the Takagi-Taupin equations.

Results and Discussion

In a CVD reactor the wafers are placed on a SiC susceptor which is mounted inside a quartz chamber. A series of halogen lamps are located on the top and down of the quartz in order to warm up the susceptor. The heat radiation is absorbed mainly by the susceptor and the substrate temperature is established. The kinetics of CVD growth can physically be described by classical boundary layer theory assuming a laminar gas flow over the wafer.¹⁶ Figure 1 illustrates a schematic view of the gas kinetics.

Due to the frictional force between the gas steam and the stationary susceptor/substrate, a stagnant boundary layer is established during the gas flow (see Figure 1). Beyond this boundary layer, the gas is assumed to be well-mixed and moving at a constant speed. Gas molecules, which have diffused through the gas boundary layer, are pulled down due to the pressure gradient between the surface and the boundary layer. They are attracted toward the dangling bonds and are then consumed. The vertical diffusion path of the gas molecules was 10–15 mm for the total pressure of 20–40 torr in an Epsilon 2000 CVD reactor.¹⁷

There are a series of publications about the physics behind the epitaxy growth of SiGe layers using the CVD technique.^{18–20} In this process, the impinging reactant molecules on the Si surface are incorporated to the dangling bonds. By applying the Maxwell distribution function in unit time, the number of the reactant molecules (Γ) which interact with a unit area of the substrate with kinetic energy above E_A can be estimated:

$$\Gamma = \frac{N_R}{(2\pi m_R k_B T)^{\frac{1}{2}}} (E_A + k_B T) \exp\left(-\frac{E_A}{k_B T}\right) \quad [1]$$

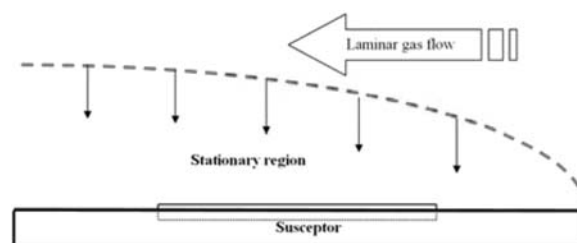


Figure 1. Schematically illustration of how classical boundary layer forms from laminar gas stream flowing over the wafer in non-selective epitaxy growth (NSEG) during the CVD process. Black arrows in this figure demonstrate the diffused molecules path to reach the dangling bonds. Si substrate is placed inside the susceptor.

^{*} Electrochemical Society Active Member.

^a Present address: Department of Electrical and Computer Engineering, Nano-Electronic Laboratory, University of Tehran, Tehran, Iran.

^z E-mail: mkcs@kth.se

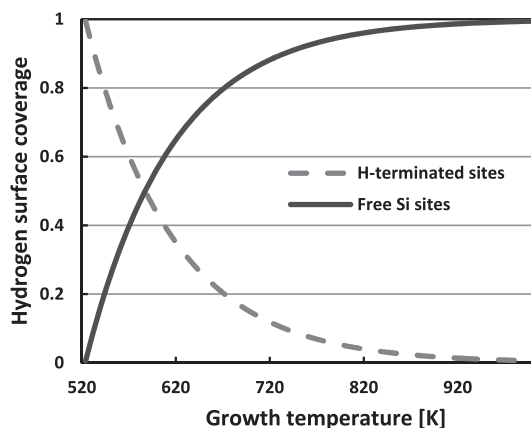


Figure 2. Surface coverage of hydrogen as a function of temperature.

where N_R is the number of reactant molecules in a unit volume of the gas phase and m_R is the mass of a reactant molecule and E_A is deposition activation energy. k_B and T are respectively Boltzmann constant and temperature. The deposition of Si layers on a Si surface is notably the simplest case of epitaxy growth. The main contributing specie in this case is the SiH_2 radical which has a unity sticking coefficient on the dangling bonds according to the previous reports.²¹ The growth rate for Si deposition can be calculated as follows:

$$R_{\text{Si}} = \frac{\Gamma}{N_0} = \beta \frac{(1 - \theta_{\text{H}(\text{Si})})}{N_0} \frac{P_{\text{Si}_2\text{H}_6}}{(2\pi m_{\text{Si}_2\text{H}_6} k_B T)^{\frac{1}{2}}} \times \left(\frac{E_{\text{Si}_2\text{H}_6}}{k_B T} + 1 \right) \exp\left(-\frac{E_{\text{Si}_2\text{H}_6}}{k_B T}\right) \quad [2]$$

where β , θ , P , m , N_0 and E are respectively: unit-less constant; surface coverage of hydrogen; partial pressure of disilane; molecular mass of disilane; number of atoms in a unit volume of the substrate layer; and activation energy needed for deposition. Activation energy of 1.56 eV was extracted practically for disilane deposition from the Arrhenius plot. The parameter β in above equation is called tooling factor which should not be considered as a fitting parameter. It presents the vertical diffusion of the molecules downwards and it obeys the Fick's law. In other words, β parameter has a physical meaning and is dependent on the reactor geometry and the distribution of gases in the reactor chamber. This parameter alters by the gas injectors.

The surface coverage of an adsorbed gas, which is temperature dependent, can be obtained through the Langmuir isotherm. For Si deposition at low temperature from disilane, the dominant reactions occur through a series of H dissociation but ultimately the following chemical reactions and adsorption can be written:²²



where $_$ is a dangling bond. The Langmuir isotherm for an equilibrium case can be written as:

$$B(T) = \frac{\theta_H^2}{P_H(1 - \theta_H)^2} \quad [3]$$

where $B(T)$ is the reaction constant and P is the hydrogen partial pressure which is close to 1. Therefore, this reaction constant can be rewritten as:

$$B(T) = \frac{\theta_H^2}{(1 - \theta_H)^2} \quad [4]$$

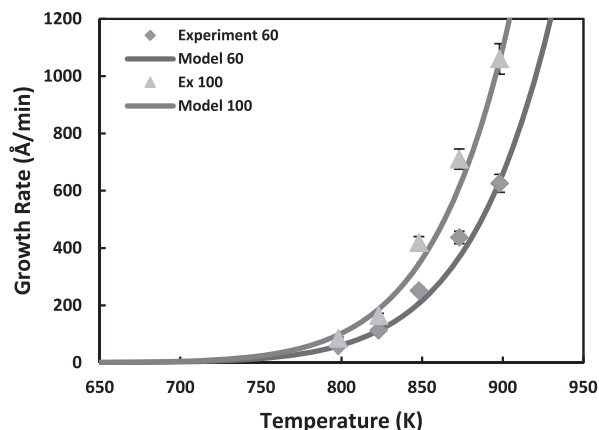


Figure 3. Growth rate of Si for two disilane partial pressure (60 and 100 mtorr) as a function of temperature.

However, epitaxy is a non-equilibrium process in which the above expression must be thus modified. Desorption of hydrogen is the limitation of the growth rate at low temperature. Basically, the deposition in LTE is limited by the availability of free surface sites. Our model in this work empirically calculates the surface coverage of hydrogen which is illustrated in Figure 2. Figure 2 shows that 50% of all surface sites are blocked with hydrogen at around 314°C. According to our calculations, 2 to 20% of the silicon sites are occupied in the temperature range chosen for this study (from 400 to 600°C).

Figure 3 depicts the Si growth rate model for two different disilane partial pressure (60 and 100 mtorr) as a function of temperature. The experimental results are also added to proof the correctness of the calculations. The nice feature in this plot is that the growth rate increases linearly with increasing the disilane partial pressure. This is due to the independency of the hydrogen surface coverage on the disilane partial pressure. Since hydrogen is the carrier gas with very high input levels in this process (slm range), changing the precursor flow (sccm range) does not affect the hydrogen amount inside the chamber.

The effect of Ge atoms on growth rate was considered by adding the digermene to the source gases. Four different partial pressures for Ge (0.5, 3, 4 and 4.9 mtorr) were used and the activation energies were calculated through the Arrhenius plots. To eliminate effects of other parameter, the disilane partial pressure was kept constant at 60 mtorr. Figure 4 illustrates the calculated activation energies vs. digermene/disilane partial pressure ratio. The results show that increasing Ge_2H_6 partial pressure decreases the total deposition activation energy. All values in this chart are less than activation energy calculated for Si deposition (1.56±0.07 eV in this figure). The presence of

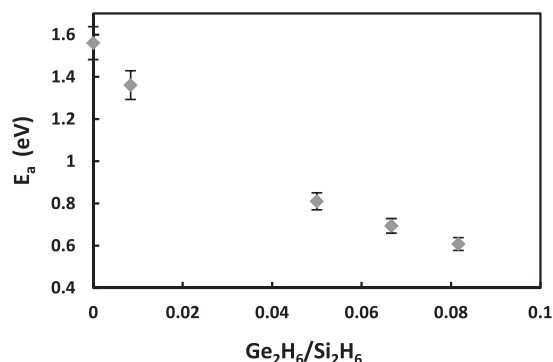


Figure 4. Activation energy of deposition vs. $\text{Ge}_2\text{H}_6/\text{Si}_2\text{H}_6$ partial pressure ratio.

Ge atoms on the surface enhances the growth rate for two reasons; first, they require lower activation energy for deposition than do Si (0.29 eV for Ge compared to 1.56 eV for Si); and second, the desorption energy of H from these atoms is also lower than Si²³ which makes them favorable desorption sites for undesired hydrogen atoms on the surface. Thus, Si atom binding becomes easier in the presence of Ge atoms.

For the modeling of LTE of SiGe, a phenomenological consideration was taken into account. This means that the total growth rate was assumed as a sum of the growth rates from different sources contributing in the epitaxy process. The total growth rate can thus be given by:

$$R_T = R_{Si} + R_{Ge} + R_{Si/Ge} + R_{Ge/Si} \quad [5]$$

where $R_{Si/Ge}$ ($R_{Ge/Si}$) relates to the Si (Ge) deposition in the presence of Ge (Si) atoms on the surface. Since Ge atoms on the surface mainly contribute to provide free sites, the term $R_{Ge/Si}$ is negligible in this equation. This means that the $R_{Si/Ge}$ is a result of R_{Ge} . Thus, they can be merged and Eq. 5 is simplified as:

$$R_T = R_{Si} + R_{Ge} + mR_{Ge} = R_{Si} + (1 + m)R_{Ge} \quad [6]$$

m in this equation is called substitution coefficient.²⁴ “ m ” is related to be the number of silyl groups which have been substituted for hydrogen atoms in digermane molecules by a chemical gas reaction. Thus, an individual molecule of the hypothetical digermane intermediate transports not only a germanium atom from the gas to the surface but also “ m ” silicon atoms which will be incorporated in the epitaxial layer. Eq. 2 represents the growth rate of Si in the epitaxy process which can simply be shown as:

$$R_{Si} = AP_{Si_2H_6} \quad [7]$$

where A includes all other parameters in Eq. 2. Similar equation can also be given for Ge growth rate:

$$R_{Ge} = BP_{Ge_2H_6} \quad [8]$$

Thus, substituting Eqs. 7 and 8 in Eq. 6 leads to the following expression:

$$\frac{R_T - R_{Si}}{R_{Si}} = \frac{(1 + m)R_{Ge}}{R_{Si}} = (1 + m) \frac{B P_{Ge_2H_6}}{A P_{Si_2H_6}} \quad [9]$$

Using this equation, the relative Ge-related growth rate can be plotted as a function of the ratio of the partial pressures of digermane and disilane. Figure 5 illustrates the results of the calculations. In this figure, the relative Ge-related growth rate is plotted for 4 different temperatures.

There are different ways of explaining the substitution coefficient.²⁵ In this case, for calculating the Ge content (x) the following simple assumption can be considered:

$$\frac{1}{x} = \frac{R_T}{R_{Ge}} = \frac{R_{Si} + (1 + m)R_{Ge}}{R_{Ge}} \quad [10]$$

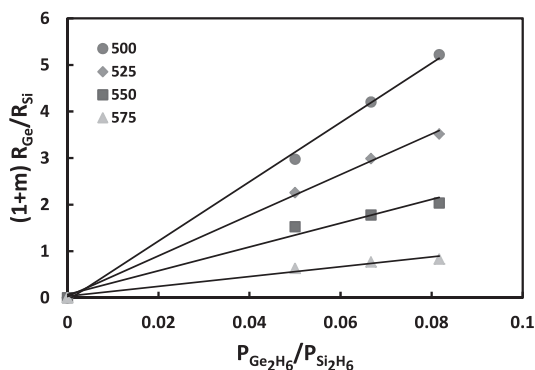


Figure 5. Relative germane-related growth rate of SiGe as a function of the ratio of the partial pressures of digermane and disilane.

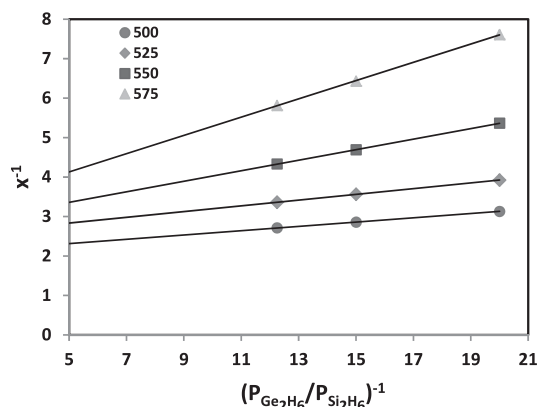


Figure 6. Inverse Ge content (x^{-1}) as a function of the inverse partial pressure ratio of digermane and disilane.

Substitution of Eqs. 7 and 8 in Eq. 10 gives:

$$\frac{1}{x} = (1 + m) + \frac{A}{B} \left(\frac{P_{Ge_2H_6}}{P_{Si_2H_6}} \right)^{-1} \quad [11]$$

The inverse germanium content (x^{-1}) versus the inverse partial pressure ratio of digermane and disilane is plotted in Figure 6. In this figure, the straight lines show that the experimental data are fairly in decent agreement with Eq. 11. The ordinate intercept of each line correlates to the inverse maximum amounts of relative Ge contents possible at the corresponding temperature.²⁵ According to this figure, at 500, 525, 550 and 575°C, the maximum Ge contents will be 49, 40, 37 and 33%, respectively.

According to Eq. 11, “ m ” can be obtained from the ordinate intercepts given in Figure 6. It can also be extracted by multiplying the slopes of corresponding temperatures in Figs. 5 and 6. This may be explained by comparing Eqs. 9 and 11. Table I summarizes the results. The average, which is shown on the last column, is more reliable. Table I just shows the integers by rounding the average numerical values.

According to this table, “ m ” in this temperature range is two which means each Ge atom is contributing in deposition of two Si atoms. Thus, using Eqs. 2 and 6, the total growth rate of SiGe epitaxy growth can be expressed by:

$$R_T = \beta \frac{(1 - \theta_{H(Si)})}{N_0} \frac{P_{Si_2H_6}}{(2\pi m_{Si_2H_6} k_B T)^{\frac{1}{2}}} \times \left(\frac{E_{Si_2H_6}}{k_B T} + 1 \right) \exp \left(-\frac{E_{Si_2H_6}}{k_B T} \right) + \chi(1 + m) \frac{(1 - \theta_{H(Si)})}{N_0} \frac{P_{Ge_2H_6}}{(2\pi m_{Ge_2H_6} k_B T)^{\frac{1}{2}}} \times \left(\frac{E_{Ge_2H_6}}{k_B T} + 1 \right) \exp \left(-\frac{E_{Ge_2H_6}}{k_B T} \right) \quad [12]$$

where χ is a unit-less tooling factor which is dependent on the gas property and the reactor geometry. It should be emphasized here that Ge deposition occurs mostly through series of Ge_2H_6

Table I. M estimation.

Temp.	$x^{-1}(0)-1$	$\tan\alpha\cot\beta-1$	m
500	1.04	2.4435191	2
525	1.47	2.1532922	2
550	1.69	2.4016827	2
575	1.97	1.452974	2

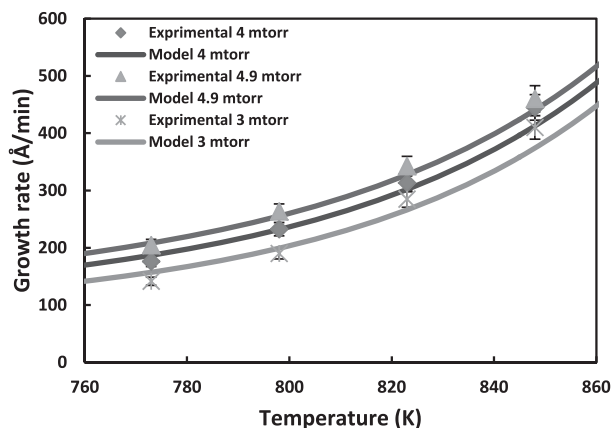


Figure 7. Growth rate of SiGe vs. temperature for different digermene partial pressures (3, 4, and 4.9 mtorr); disilane partial pressure was 60 mtorr.

dissociations and adsorption of GeH_2 radicals on the surface. R1, R2 and R3 can also be written using digermene parameters. Finally, the experimental and calculated results from Eq. 12 are shown in Figure 7. Four different temperatures and three different GeH_4 partial pressures have been used to prove the sanity of the model. This figure shows a fairly good concurrence between the model and experimental data.

The Ge content in SiGe layers is also an important factor for the strain and bandgap calculations. It can be obtained from the flux/partial pressure ratio between Ge and Si¹³ as shown in the following equation:

$$\frac{x^2}{1-x} = \alpha \left(\frac{P_{\text{Ge}_2\text{H}_6}}{P_{\text{Si}_2\text{H}_6}} \right) \quad [13]$$

where x is the Ge content. α is the result of adsorption and desorption of the main species involved in the deposition:

$$\alpha = \frac{k_{a,\text{GeH}_2} \times k_{d,\text{H}}}{k_{a,\text{SiH}_2} \times k_{d,\text{H}}} = \frac{k_{a,\text{GeH}_2}}{k_{a,\text{SiH}_2}} = A \exp\left(\frac{E}{k_B T}\right) \quad [14]$$

The adsorption energy difference in Eq. 8 ($E_{a,\text{SiH}_2} - E_{a,\text{GeH}_2}$) is empirically calculated to be 1.43 eV. The results of the model and measured data are illustrated in Figure 8. It is clear that by decreasing the growth

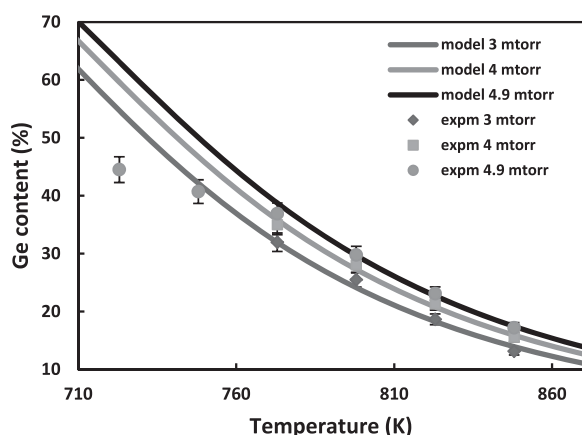


Figure 8. Ge content (%) of the SiGe layers vs. the growth temperature for different digermene partial pressure (3, 4, and 4.9 mtorr); disilane partial pressure was 60 mtorr.

temperature, Ge content increases. If an epitaxy growth process continues long enough that the epi-film reaches the critical thickness, it begins to relax.²⁶

This can be seen in this figure at temperatures below 773 K. At these temperatures by using 4.9 mtorr Ge_2H_6 , the experimental result is located below the model lines. This is because the thickness of SiGe layer (e.g. 818 Å at 773 K) exceeds the critical thickness. It is worth mentioning here that 37% as shown in this figure is not the highest limit for the Ge content. Layers with even higher Ge contents can be grown using these sources but with a thickness which is located in the meta-stable growth region.

Conclusions

An empirical model for $\text{Si}_2\text{H}_6/\text{Ge}_2\text{H}_6$ -based epitaxy growth of SiGe at LTE was presented. The growth rate of Si and SiGe was calculated by considering the number of free sites and impinging atoms to the surface at a certain temperature. The activation energy for the chemical reactions were estimated from the experimental data. The Ge content in epi-layers was also calculated and compared with the experimental data. A good agreement between the model and experimental data was found.

References

- K. Goto, J. Murota, T. Maeda, R. Schuetz, K. Aizawa, R. Kircher, K. Yokoo, and S. Ono, *Japanese Journal of Applied Physics*, **32**, 438 (1993).
- S. Verdonckt-Vandebroek, E. F. Crabbe, B. S. Meyerson, D. L. Harnam, P. J. Restle, J. M. C. Stork, and J. B. Johnson, *IEEE Transactions on Electron Devices*, **41**, 90 (1994).
- A. Lindgren, P. Hellberg, M. Von Haartman, D. Wu, C. Menon, S. Zhang, and M. Östling, in: *ESSDERC 2002. Proceedings of the 32nd European Solid-State Device Research Conference*, Firenze, Italy, 2002, pp. 175–8.
- A. Gupta, S. P. Levitan, L. Selavo, and D. M. Chiarulli, in: *17th International Conference on VLSI Design. Proceedings*, IEEE Comput. Soc, 2004, pp. 957–960.
- M. Kolahdouz, A. Afshar Farniya, L. Di Benedetto, and H. Radamson, *Applied Physics Letters*, **96**, 213516 (2010).
- H. H. Radamson, M. Kolahdouz, S. Shayestehaminzadeh, A. Afshar Farniya, and S. Wissmar, *Applied Physics Letters*, **97**, 223507 (2010).
- M. Strasser, R. Aigner, M. Franosch, and G. Wachutka, *Sensors And Actuators A*, **97–98**, 535 (2002).
- M. Wagner, G. Span, and T. Grasser, in: *International SiGe Technology and Device Meeting*, Ieee, 2006, pp. 1–2.
- N. Tamura and Y. Shimamura, *Applied Surface Science*, **254**, 6067 (2008).
- S. E. Fischer, R. K. Cook, R. W. Knepper, R. C. Lange, K. Nummy, D. C. Ahlgren, M. Revitz, and B. S. Meyerson, in: *Technical Digest - International Electron Devices Meeting*, 1989, pp. 890–892.
- A. Vonsovici, L. Vescan, and S. P. Pogossian, in: *58th DRC. Device Research Conference. Conference Digest (Cat. No. 00TH8526)*, Ieee, 2000, pp. 49–50.
- J. F. Damlencourt, *ECS Transactions*, **28**(1), 343 (2010).
- T. Kuijter, L. J. Giling, and J. Bloem, *Journal of Crystal Growth*, **22**, 29 (1974).
- K. L. Knutson, R. W. Carr, W. H. Liu, and S. A. Campbell, *Journal of Crystal Growth*, **140**, 191 (1994).
- B. Mehta and M. Tao, *Journal of The Electrochemical Society*, **152**, G309 (2005).
- M. Kolahdouz, L. Maresca, M. Ostling, D. Riley, R. Wise, and H. Radamson, *Solid-State Electronics*, **53**, 858 (2009).
- J. Hallstedt, M. Kolahdouz, R. Ghandi, H. Radamson, and R. Wise, *Journal of Applied Physics*, **103**, 0549071 (2008).
- M. Kolahdouz, L. Maresca, R. Ghandi, A. Khatibi, and H. H. Radamson, *Journal of The Electrochemical Society*, **158**, H457 (2011).
- H. H. Radamson, W. Ni, and G. V. Hansson, *Applied Surface Science*, **102**, 82 (1996).
- M. Tao, *Thin Solid Films*, **223**, 201 (1993).
- T. Zhang, P. Zhang, C. K. Law, and F. Qi, *Chemical Vapor Deposition*, **15**, 274 (2009).
- D. W. Greve, *Materials Science and Engineering: B*, **18**, 22 (1993).
- H. Kim, P. Desjardins, J. Abelson, and J. Greene, *Physical Review B*, **58**, 4803 (1998).
- H. Kühne and T. Morgenstern, *Crystal Research and Technology*, **27**, 773 (1992).
- H. Kühne, *Journal of Crystal Growth*, **125**, 291 (1992).
- M. Kolahdouz, P. T. Z. Adibi, A. A. Farniya, S. Shayestehaminzadeh, E. Trybom, L. Di Benedetto, and H. Radamson, *Journal of The Electrochemical Society*, **157**, H633 (2010).